Oxidation and Photo-Oxidation of Water on TiO2 Surface

ARTICLE *in* THE JOURNAL OF PHYSICAL CHEMISTRY C · JUNE 2008

Impact Factor: 4.77 · DOI: 10.1021/jp711929d

Oxidation and Photo-Oxidation of Water on TiO_2 Surface

Á. Valdés,* Z.-W. Qu, and G.-J. Kroes

LIC, Gorlaeus Laboratoria, Universiteit Leiden, 2300 RA Leiden, The Netherlands

J. Rossmeisl and J. K. Nørskov

Center for Atomic-Scale Materials Design, Department of Physics, Nano-DTU, Technical University of Denmark, 2800 Kgs. Lyngby, Denmark

Received: December 20, 2007; Revised Manuscript Received: April 11, 2008

The oxidation and photo-oxidation of water on the rutile TiO_2(110) surface is investigated using density functional theory (DFT) calculations. We investigate the relative stability of different surface terminations of TiO_2 interacting with H_2O and analyze the overpotential needed for the electrolysis and photoelectrolysis of water. We found that the most difficult step in the splitting of water process is the reaction of a H_2O molecule with a vacancy in the surface to form an adsorbed hydroxyl group (OH*). Comparison to experiment shows that the computed overpotential for O_2 evolution (0.78 V) is available under the experimental conditions required for both oxygen and hydrogen evolution.

1. Introduction

The photoelectrolysis of water at the surface of semiconductor metal oxides has attracted much attention in the last decades since the pioneering work of Fujishima and Honda on TiO_2.[1] This process provides hydrogen as a clean and sustainable carrier of solar energy.[2] Most of the studies on solar hydrogen are concentrated on the development of photoelectrochemical cells that involve a semiconductor photoanode and a metal cathode inmersed in an electrolyte. The process results in oxygen evolution at the photoanode and hydrogen evolution at the cathode. Unfortunately, the reaction at the photoanode is associated with substantial energy loss, mainly due to high overpotentials at the oxygen-evolving anode.

The most frequently studied material for the photoanode is TiO_2. Despite its large band gap (3 eV in the rutile phase), larger than that for other semiconductor materials such us WO_3 or Fe_2O_3, TiO_2 has become a benchmark material for understanding the photo-oxidation process in the water-splitting reaction.[1,3–26] The wide band gap of TiO_2 is out of the visible light region, which makes the final photoenergy conversion factor less than 1%.[27]

For this reason, new classes of semiconductor materials are continuously being tested in order to use the less energetic but more abundant visible light.[28–32] Recent results on titanium disilicide suggest that an efficiency of about 4% can be reached for silicide semiconductors, the band gap of which varies from 1.5 to 3.4 eV, and that their poor stability can be overcome by covering them with an oxide layer.[33]

Another option to extend the photoactivity to visible light is the use of tandem cells consisting of two photosystems connected in series.[34,35] In these devices, a thin film of nanocrystalline WO_3[36] or Fe_2O_3[37,38] serves as the top electrode absorbing the blue part of the solar spectrum and acting as a catalyst for the photo-oxidation of water. The electrons that originated in this film are then fed to a second photosystem consisting of a dye-sensitized nanocrystalline TiO_2 electrode which captures the red and green part of the solar spectrum and enables hydrogen to be generated by the conduction band electrons.

Some advantages of the TiO_2 semiconductor catalyst are that it is cheap and chemically and biologically inert and that it is very stable under illumination for water photolysis. Moreover, the photoactivity of TiO_2 can possibly be extended from the ultraviolet to the visible part of the solar radiative field by chemical doping[20,39–44] or by using TiO_2 nanotube arrays.[45]

The rutile TiO_2 crystal is the thermodynamically most stable form under ambient conditions, and the rutile (110) surface has been considered as a prototype system in surface science studies of metal oxides and oxide-supported catalysts.[14,46] To improve the efficiency of photocatalysts for water oxidation, it is very important to understand the mechanism of the oxidation of water on oxide surfaces, especially the involved chemical steps that could be related to the high oxygen-evolving overpotential. In a previous work, the O_2-evolving overpotential was studied for electrolysis on three rutile-type oxides (RuO_2, IrO_2, and TiO_2),[47] determining that the trend of overpotentials can be writen as $RuO_2 < IrO_2 < TiO_2$. For TiO_2, an overpotential of 1.19 V was found for a TiO_2 surface with a termination with oxygen present as bridging O atoms but on which the coordinatively unsaturated Ti atoms were not covered by oxygen.

The aim of this article is to study the oxidation and photo-oxidation of water on the rutile TiO_2 surface. We first study different oxygen coverages of the surface in contact with H_2O and their relative stability as a function of the applied bias and the pH of the electrolyte and then analyze the reaction mechanisms of the oxidation of water on the surfaces that are stable over a particular range of bias and pH values, according to the thermochemistry of the reactions. We consider reaction mechanisms including a OOH* intermediate on a defect-free surface.[16,19] The interaction of the active site species with the neighboring absorbed water molecules has not been taken into account in our model, as further discussed below.

To study the photo-oxidation, we assume that the driving force for the reaction at the anode is provided by holes at the upper edge of the valence band of a rutile TiO_2(110) surface

* To whom correspondence should be addressed. E-mail: avdeluxan@chem.leidenuniv.nl.

10.1021/jp711929d CCC: $40.75
Published on Web 06/11/2008

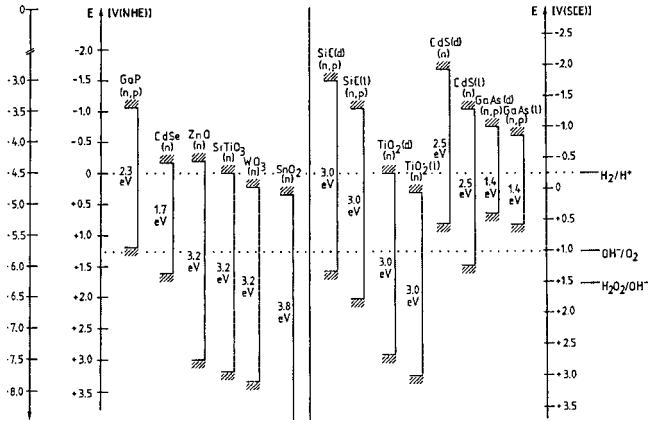

Figure 1. Position of energy bands at the surface of various semiconductors at pH = 0; (d) dark, (l) Illuminated. Reprinted with permission from J. Phys. Chem. 1996, 100, 13061−13078. Copyright 1996 American Chemical Society.

under irradiation. The redox potential for the photogenerated holes, according to the photoelectrochemical studies discussed in refs 48 and 49 (see also Figure 1) is 3.25 V versus the normal hydrogen electrode (NHE) for rutile TiO_2 at pH = 0. In a sense, the definite bias corresponding to illumination makes the study of photo-oxidation (photoelectrolysis) easier than the study of mere oxidation (electrolysis). As expressed by Figure 1, photo-oxidation corresponds to a definite bias imposed by shining light on the photoanode, and the only question to be addressed is whether this bias provides enough overpotential for the oxidation of H_2O at the imposed pH.

For electrolysis, on the other hand, a range of surfaces corresponding to a range of bias values at the given pH needs to be investigated because the overpotential may depend on the particular surface termination (O coverage) that is stable at a given bias value, which can be freely imposed when doing electrolysis.

The structure of the article is as follows: in section 2, we analyze the reaction mechanism of the water-splitting reaction for the different surface terminations, in section 3, the method to calculate the free-energy differences between the different reaction steps is explained, and in section 4, the results of the calculations on the relative stability of the different surface terminations and on the reaction mechanism steps are presented. Finally, in section 5, these results are discussed, and the conclusions are presented in section 6.

2. Water-Splitting Reaction

The water splitting reaction can be written as

Anode:

$$H_2O \rightarrow 1/2O_2 + 2H^+ + 2e^- \quad (1)$$

Cathode:

$$2H^+ + 2e^- \rightarrow H_2 \quad (2)$$

We investigate different reaction mechanisms at the anode depending on the surface termination of the TiO_2(110) face. We consider two different surface terminations that could be relevant for the water oxidation process (see Figure 2). The surfaces are the one with all bridge sites occupied by oxygen, S^1 ($TiO_2 + 2O_b$), and the totally O covered surface, S^2 ($TiO_2 + 2O_b + 2O^*$), where the coordinatively unsaturated sites (CUSs, the surface Ti atoms not covered by oxygen) are also covered by oxygen. O_b represents a bridging oxygen atom, * represents the CUS site where the reaction takes place, and O* is an oxygen atom adsorbed to a CUS site.

In our model, we assume that the reaction proceeds through one-electron transfer steps. We label the reaction steps as A, B, C, and D depending on which of the next reactions are involved:

- A: $H_2O + * \rightarrow HO^* + H^+ + e^-$
- B: $HO^* \rightarrow O^* + H^+ + e^-$
- C: $H_2O + O^* \rightarrow HOO^* + H^+ + e^-$
- D: $HOO^* \rightarrow O_2 + * + H^+ + e^-$

The reaction sequences studied for each surface are

Surface: S^1 ($TiO_2 + 2O_b$)

$$2H_2O + * \xrightarrow{A} HO^* + H_2O + H^+ + e^- \xrightarrow{B} O^* + H_2O + 2H^+ + 2e^- \xrightarrow{C} HOO^* + 3H^+ + 3e^- \xrightarrow{D} O_2 + * + 4H^+ + 4e^- \quad (3)$$

The above sequence starts with the reaction of a water molecule with a free CUS site leading to OH* at the CUS site.

Surface: S^2 ($TiO_2 + 2O_b$) + 2O*

$$2H_2O + O^* \xrightarrow{C} HOO^* + H_2O + H^+ + e^- \xrightarrow{D} O_2 + H_2O + * + 2H^+ + 2e^- \xrightarrow{A} O_2 + HOO^* + 3H^+ + 3e^- \xrightarrow{B} O_2 + O^* + 4H^+ + 4e^- \quad (4)$$

This sequence starts with reaction of O* at a CUS site with H_2O leading to OOH*.

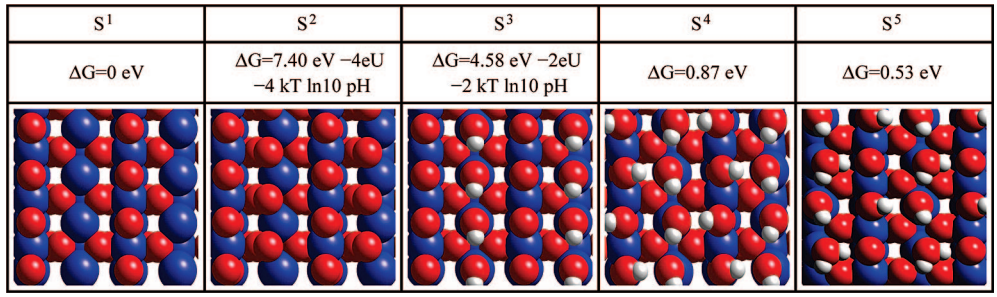

Figure 2. Plot of the different surfaces studied. S^1 represents the surface with all bridge sites occupied by oxygen, S^2 represents the totally O* covered surface, S^3 is the surface with oxygen in the bridge sites and HO* in the CUS sites, S^4 is the totally HO* covered one, and S^5 represents the surface that alternates nondeprotonated and deprotonated adsorbed water. Blue spheres represent metal ions, red spheres represent oxygen, and white spheres represent hydrogen.

TABLE 1: Zero-Point Energy Corrections and Entropic Contributions to Free Energies

	TS	ZPE
H_2O	0.67 (0.035 bar)	0.56
$OOH^* + 3/2H_2$	0.62	0.82
$OH^* + 1/2H_2$	0.20	0.49
$O^* + H_2$	0.41	0.32
$1/2O_2 + H_2$	0.73	0.32
H_2	0.41	0.27
$1/2\ O_2$	0.32	0.05
O*	0	0.05
OH*	0	0.35
OOH*	0	0.41
H_2O^*	0	0.70
O_b	0	0.08
OH_b	0	0.38

TABLE 2: Components of the Free-Energy Changes (eV) in the Relative Stability Calculation of the Different Surface Terminations

	E(eV)
$\Delta E_{R_1} = E_{S^2} - E_{S^1}$	−867.96
$\Delta E_{R_2} = E_{S^3} - E_{S^1}$	−903.55
$\Delta E_{R_3} = E_{S^4} - E_{S^1}$	−940.01
$\Delta E_{R_4} = E_{S^5} - E_{S^1}$	−940.42
E_{H_2}	−32.03
E_{H_2O}	−469.69
$(\Delta ZPE - T\Delta S)_{R_1}$	0.04
$(\Delta ZPE - T\Delta S)_{R_2}$	0.78
$(\Delta ZPE - T\Delta S)_{R_3}$	1.52
$(\Delta ZPE - T\Delta S)_{R_4}$	1.57

TABLE 3: Change of the Free Energy Coming from the Differences in Zero-Point Energies, ΔZPE, and the Change in Entropy ΔS for the Different Reaction Steps

$H_2O + * \rightarrow HO^* + 1/2H_2$	$HO^* \rightarrow O^* + 1/2H_2$	$H_2O + O^* \rightarrow HOO^* + 1/2H_2$	$HOO^* \rightarrow O_2 + * + 1/2H_2$
$(\Delta ZPE - T\Delta S)_A$	$(\Delta ZPE - T\Delta S)_B$	$(\Delta ZPE - T\Delta S)_C$	$(\Delta ZPE - T\Delta S)_D$
0.40	−0.37	0.39	–0.42

We only consider reaction steps involving one-electron transfer, which depend directly on the applied potential. The diffusion of species and other surface reactions is expected to depend only weakly on the potential. We consider a mechanism on the anode where the oxygen molecules are formed via a surface HOO* intermediate and the reaction takes place at the CUS sites. Direct recombination of oxygen atoms to form O_2 is not considered because a large activation barrier can be expected for that process.[50] For each of the surfaces, we will analyze the potential range at which all steps become thermodynamically possible at a given pH. This way, the overpotential needed for the electrolysis is computed for each surface termination to evaluate whether electrolysis may take place for that surface termination over the range of biases at which it is stable. We also determine whether the photo-oxidation of H_2O may proceed spontaneously at the potential corresponding to illumination of a TiO_2 photoanode for the surface that is stable at this potential and at the pH imposed.

3. Method

We use the method developed in ref 51 that concentrates on the thermochemistry of the reaction. In this method, the discussion of energy barriers for the different elementary steps is restricted to the barriers that come from differences of free energies of the intermediates. Kinetic barriers between intermediates may also play a role, but this is not included in the model. The approach described below allows one to determine whether the intermediate one-electron transfer reaction steps are thermodynamically allowed, which is a necessary (but not sufficient) criterion for the reaction to proceed.

The method to obtain the free-energy differences between the intermediates can be summarized as follows:

(1) To calculate the free energy of the intermediates when they include $H^+ + e^-$, we consider the reference potential to be that of the standard hydrogen electrode (NHE). Then, we can relate the chemical potential for $H^+ + e^-$ to that of 1/2 H_2 in the gas phase. That means that at pH = 0, p = 1 bar, and T = 298 K, the free energy of $H^+(aq) + e^-$ can be taken equal to that of 1/2 H_2. Then, at standard conditions (U = 0, pH = 0, p = 1 bar, T = 298 K), $\Delta G_0 = \Delta G$ of the reaction $*AH \rightarrow A + H^+ + e^-$ is equivalent to that of the reaction $*AH \rightarrow A + 1/2\ H_2$.

(2) $\Delta G_0 = \Delta E + \Delta ZPE - T\Delta S$ is calculated as follows: The reaction energy ΔE is calculated using density functional theory (DFT). The differences in zero-point energies, ΔZPE, and the change in entropy ΔS are calculated using DFT calculations of vibrational frequencies and using standard tables for gas-phase molecules.[52] We assume that $S = 0$ for the atoms and molecules adsorbed to the CUS site. The temperature dependence of the enthalpy is neglected in the calculations (we assume $\Delta H(298\ K) = \Delta H(0\ K)$).

(3) We include the effect of a potential bias on all states involving one electron in the electrode by shifting the energy of this state by $\Delta G_U = -eU$, where U is the electrode potential relative to the standard hydrogen electrode.

(4) At a pH ≠ 0 we can correct the free energy of H^+ ions by the concentration dependence of the free energy: $\Delta G_{pH}(pH) = -kT \ln 10 \cdot pH$.

An effect of pH not considered here is that, below the isoelectric point (that is between pH = 4.8 and 5.5 for rutile $TiO_2(110)$),[53] the surface is partially protonated, while above this value, it will be partially covered by OH^-. This could affect the adsorption energy of the modeled species, but taking this effect into account would require too large unit cells and was not done here.

(5) The DFT values of the energy of H_2O and H_2 in the gas phase are used as references states since they are well described within DFT. The entropy of gas-phase water is calculated at 0.035 bar because this is the equilibrium pressure at room temperature. This means that the free energy of gas-phase water at these conditions is equal to the free energy of liquid water.

The free-energy change of the total reaction $H_2O \rightarrow 1/2\ O_2 + H_2$ is fixed at the experimentally found value of 2.46 eV per water molecule. This is done in order to avoid DFT calculations of O_2 since this molecule has a complicated electronic structure, which is not described accurately with DFT. This means that in the reaction step involving the formation of O_2, we consider that $\Delta G_{\{2H_2O \rightarrow O_2 + 2H_2\}} = 4.92\ eV = E_{O_2} + 2E_{H_2} - 2E_{H_2O} + (\Delta ZPE - T\Delta S)_{\{2H_2O \rightarrow O_2 + 2H_2\}}$.

(6) In the calculation of the electronic energies of the intermediates, the interaction with neighboring water molecules can also be taken into account. However, this was not yet done here. We assume that the interaction energy of water with O*, OH*, OOH*, or an empty CUS site is similar, approximately equal to the energy of a hydrogen bond. Moreover, this effect was found to be negligible for similar rutile-type oxides.[47]

The DFT calculations of the reaction energies are performed using a plane wave implementation[54] at the generalized gradient approximation (GGA) RPBE level.[55] A periodically repeating

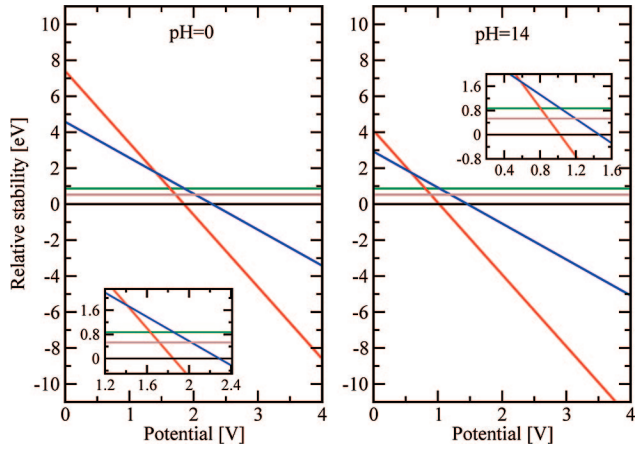

Figure 3. The phase diagram of the $H_2O + TiO_2(110)$ surface system calculated as function of the potential at pH = 0/14. We compare the free energy of the surface with all bridge sites occupied with O, S^1 ($\Delta G = 0$, black line), with the fully O-covered surface, S^2 (red line), the surface with oxygen in the bridge sites and HO* in the CUS sites, S^3 (blue line), the surface fully covered by HO, S^4 (green line), and the surface that alternates dissociated and molecularly adsorbed water, S^5 (brown line). The free energy of two CUS sites in the 2 × 1 surface unit cell plus two water molecules (i.e., the energy of the S^1 surface) is taken as energy zero.

four-layer slab is chosen for the most stable rutile-type (110) surface in our calculations. A vacuum of at least 20 Å is used to separate the slab from its periodic images. We use the 2 × 1 surface unit cell and the 2 × 2 × 1 Monkhorst−Pack type of k-point sampling for slab calculations. The two bottom layers of the slab are fixed at the optimized bulk lattice constants, while the two top layers as well as possible adsorbates on it are fully relaxed. Ultrasoft pseudopotentials are used to deal with the ion cores.[56] The electronic wave functions can be represented well by a plane wave basis set with a cutoff energy of 340 eV. The electron density is treated on a grid corresponding to a plane wave cutoff at 500 eV. A Fermi smearing of 0.1 eV and Pulay mixing are used to ensure the fast convergence of the self-consistent electron density. Atomic positions are relaxed until the sum of the absolute forces is less than 0.05 eV/Å. All calculations are performed using the atomic simulation environment (ASE) package.[57]

4. Results

4.1. Surface Termination. To calculate the relative stability of different surface coverages by O and OH relevant to electrolysis, we have considered the reaction free-energy changes of the following reactions

$$R_1 : S^1 + 2H_2O \leftrightarrow S^2 + 4(H^+ + e^-) \quad (5)$$

$$R_2 : S^1 + 2H_2O \leftrightarrow S^3 + 2(H^+ + e^-) \quad (6)$$

$$R_3 : S^1 + 2H_2O \leftrightarrow S^4 \quad (7)$$

$$R_4 : S^4 + 2H_2O \leftrightarrow S^5 \quad (8)$$

where S^1 and S^2 refer to the surface terminations explained above ($TiO_2 + 2O_b$) and ($TiO_2 + 2O_b + 2O^*$), respectively, S^3 refers to the surface with oxygen in the bridge sites and HO* in the CUSs, ($TiO_2 + 2O_b + 2HO^*$), and S^4 refers to the totally OH covered surface ($TiO_2 + 2HO_b + 2HO^*$). We also include the comparison with the S^5 surface that alternates nondeprotonated and deprotonated adsorbed water (see Figure 2) and that, acoording to Lindan et al., is the most stable one.[64] Note that the reaction free energies of the third and fourth reactions (R_3 and R_4) do not depend on the applied potential U, and the other two do.

The reaction free energies of the proposed reactions are

$$\Delta G_{R_1} = \Delta E_{R_1} + 2E_{H_2} - 2E_{H_2O} + (\Delta ZPE - T\Delta S)_{R_1} - 4eU - 4kT \ln 10 \cdot pH$$

$$= 7.40\ eV - 4eU - 4kT \ln 10 \cdot pH$$

$$\Delta G_{R_2} = \Delta E_{R_2} + E_{H_2} - 2E_{H_2O} + (\Delta ZPE - T\Delta S)_{R_2} - 2eU - 2kT \ln 10 \cdot pH$$

$$= 4.58\ eV - 2eU - 2kT \ln 10 \cdot pH$$

$$\Delta G_{R_3} = \Delta E_{R_3} - 2E_{H_2O} + (\Delta ZPE - T\Delta S)_{R_3} = 0.87\ eV$$

$$\Delta G_{R_4} = \Delta E_{R_4} - 2E_{H_2O} + (\Delta ZPE - T\Delta S)_{R_4} = 0.53\ eV$$

ΔE_{R_i}, with $i = 1, 2, 3$, and 4, are the energy differences between S^1 and S^2, S^3, S^4, and S^5, respectively. $(\Delta ZPE - T\Delta S)_{R_1}$, $(\Delta ZPE - T\Delta S)_{R_2}$, $(\Delta ZPE - T\Delta S)_{R_3}$, and $(\Delta ZPE - T\Delta S)_{R_4}$ are calculated from the values of Table 1.

Note that, in this work, the ZPE values of O*, OH*, and OOH* were calculated by performing calculations on $TiO_2(110)$ with O, OH, and OOH adsorbed to a CUS site, in contrast to the work reported in ref 47. In Table 2, we present the different components of the free-energy changes.

In Figure 2, we present some plots of the different surfaces, and in Figure 3, we represent the relative stability of the surfaces as a function of the applied potential U at pH = 0 and 14. Below 1.85/1.00 V, the S^1 is the most stable surface; above these values of the bias, the relevant surface is S^2 for pH = 0/14. Note that, as they are not thermodynamically favored for any value of the applied potential U, the S^3, S^4, and S^5 surfaces do not play a role in the subsequent calculations.

It should be noted that in S^2, the oxygen atoms are not adsorbed directly above the CUS sites but form bonds to CUS sites as well as surface oxygen atoms. A similar peroxo geometry was found in calculations on the adsorption of oxygen atoms to S^1 at coverages of 0.33−1 ML.[26] The depicted geometry should be relevant for situations when there is no

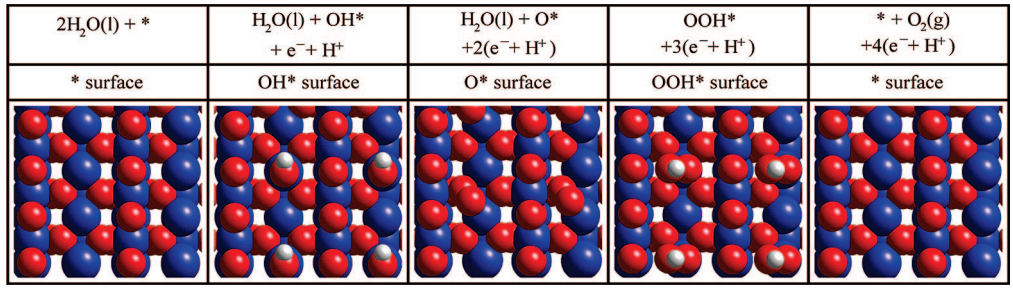

Figure 4. Structures of the intermediates of the oxygen evolution reaction on the $TiO_2(110)$ surface with all bridge sites occupied by oxygen (S^1). Blue spheres represent metal ions, red spheres represent oxygen, and white spheres represent hydrogen.

excess of electrons at the surface (under conditions pertinent to oxidation or photo-oxidation of water, there should be an excess of holes). The geometry used earlier to study the electrolysis of water on TiO_2[47] should, instead, be relevant when there is an excess of electrons at the surface.[58,59]

Our finding that H_2O does not dissociate completely on the (110) surface (resulting in S_4) or partially (resulting in S_5) is in agreement with the overview discussion of the behavior of H_2O on rutile (110) in the review paper of Diebold, where it is stated that most research agrees that H_2O only dissociates at defects.[14]

4.2. Reaction Mechanisms. In this section, the water oxidation reaction steps for each surface coverage and the corresponding free-energy changes under an applied potential U and pH are presented.

The values ($\Delta ZPE - T\Delta S$) for each step are calculated from the values from Table 1 and presented in Table 3. ΔE_X^i are the energy differences between the surface states involved in each step (X = A, B, C, D) for S^i (i = 1, 2). These values are summarized in Table 4. The changes of the free energy at standard conditions, ΔG_0, are presented in Table 5.

4.2.1. S^1 (TiO_2 + $2O_b$). We first consider the S^1 surface, where the CUS sites are originally not covered. The reaction intermediates for this surface are plotted in Figure 4. The H_2O + O* intermediate has been discussed in ref 26; see also section 4.1.

$$1.\ 2H_2O + * \xrightarrow{A} H_2O + HO^* + H^+ + e^-$$

$$\Delta G_A^1 = \Delta E_A^1 + 1/2E_{H_2} - E_{H_2O} + (\Delta ZPE - T\Delta S)_A - eU - kT \ln 10 \cdot pH$$
$$= 2.20\ eV - eU - kT \ln 10 \cdot pH$$

$$2.\ H_2O + HO^* + H^+ + e^- \xrightarrow{B} H_2O + O^* + 2(H^+ + e^-)$$

$$\Delta G_B^1 = \Delta E_B^1 + 1/2E_{H_2} + (\Delta ZPE - T\Delta S)_B - eU - kT \ln 10 \cdot pH$$
$$= 1.47\ eV - eU - kT \ln 10 \cdot pH$$

TABLE 4: Reaction Energies Differences ΔE_X^i (eV) between the Different Surface States of the Different Steps (X = A, B, C, D) in the Water Oxidation Process For the Relevant TiO_2 Surface Terminations (S^i, i = 1, 2)

	$S^{i=1}$	$S^{i=2}$
$\Delta E_A^i = E_{HO^*}^i - E_*^i$	−451.88	−452.07
$\Delta E_B^i = E_{O^*}^i - E_{HO^*}^i$	17.85	18.16
$\Delta E_C^i = E_{HOO^*}^i - E_{O^*}^i$	−452.51	−452.53
$\Delta E_D^i = E_*^i - E_{HOO^*}^i$	886.54	886.43

TABLE 5: Change of the Free Energy at Standard Conditions, ΔG_0 (eV) for the Relevant TiO_2 Surface Terminations in the Water Oxidation Process

Step	$S^{i=1}$	$S^{i=2}$
ΔG_0^i(A)	2.20	2.01
ΔG_0^i(B)	1.47	1.77
ΔG_0^i(C)	1.55	1.54
ΔG_0^i(D)	−0.30	−0.40

$$3.\ H_2O + O^* + 2(H^+ + e^-) \xrightarrow{C} HOO^* + 3(H^+ + e^-)$$

$$\Delta G_C^1 = \Delta E_C^1 + 1/2E_{H_2} - E_{H_2O} + (\Delta ZPE - T\Delta S)_C - eU - kT \ln 10 \cdot pH$$
$$= 1.55\ eV - eU - kT \ln 10 \cdot pH$$

$$4.\ HOO^* + 3(H^+ + e^-) \xrightarrow{D} O_2 + * + 4(H^+ + e^-)$$

$$\Delta G_D^1 = 4.92\ eV + \Delta E_D^1 - 3/2E_{H_2} + 2E_{H_2O} + (\Delta ZPE - T\Delta S)_D - eU - kT \ln 10 \cdot pH$$
$$= -0.30\ eV - eU - kT \ln 10 \cdot pH$$

The free energies of the intermediates are plotted in Figure 5 at pH = 0 and 14 for different U values. The rate-limiting step is step A

$$H_2O + * \xrightarrow{A} HO^* + H^+ + e^-$$

4.2.2. S^2 (TiO_2 + $2O_b$ + $2O^*$). In this case, the CUS sites are originally covered by oxygen. The reaction intermediates for this surface are plotted in Figure 6.

$$1.\ 2H_2O + * \xrightarrow{C} H_2O + OOH^* + H^+ + e^-$$

$$\Delta G_C^2 = \Delta E_C^2 + 1/2E_{H_2} - E_{H_2O} + (\Delta ZPE - T\Delta S)_C - eU - kT \ln 10 \cdot pH$$
$$= 1.54\ eV - eU - kT \ln 10 \cdot pH$$

Note that the difference between ΔG_C^2 and ΔG_C^1 above is due to the neighboring CUS sites being filled with O* or being empty, depending on the surface termination studied, leading to different interactions of HOO* and O* with the surface.

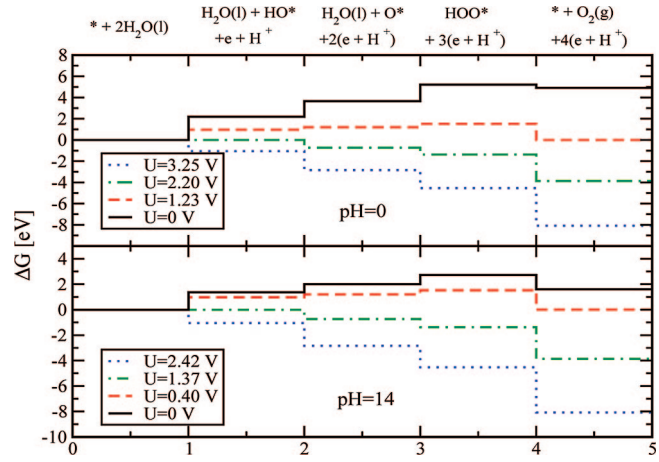

Figure 5. The free energies of the intermediates on the S^1 surface termination at pH = 0/14 (U = 0, 1.23/0.40, and 2.20/1.37 V) are depicted. At the equilibrium potential (U = 1.23/0.40 V), some reaction steps are uphill in free energy. At 2.20/1.37 V, all reaction steps are downhill in free energy at pH = 0/14. We also compare to the case with U = 3.25/2.42 V the corresponding values of the redox potential versus NHE for the photogenerated holes in the valence band of TiO_2 (rutile) in contact with H_2O under intense irradiation at pH = 0/14.

$$2.\ H_2O + OOH^* + H^+ + e^- \xrightarrow{D} H_2O + O_2 + * +$$

$$2(H^+ + e^-)$$

$$\Delta G_D^2 = 4.92\text{eV} + \Delta E_D^2 - 3/2E_{H_2} + 2E_{H_2O} + (\Delta\text{ZPE} - T\Delta S)_D - eU - kT \ln 10 \cdot \text{pH}$$

$$= -0.40\text{eV} - eU - kT \ln 10 \cdot \text{pH}$$

$$3.\ H_2O + O_2 + * + 2(H^+ + e^-) \xrightarrow{A} HO^* + O_2 +$$

$$3(H^+ + e^-)$$

$$\Delta G_A^2 = \Delta E_A^2 + 1/2E_{H_2} - E_{H_2O} + (\Delta\text{ZPE} - T\Delta S)_A - eU - kT \ln 10 \cdot \text{pH}$$

$$= 2.01\text{eV} - eU - kT \ln 10 \cdot \text{pH}$$

$$4.\ HO^* + O_2 + 3(H^+ + e^-) \xrightarrow{B} O^* + O_2 + 4(H^+ + e^-)$$

$$\Delta G_B^2 = \Delta E_B^2 + 1/2E_{H_2} + (\Delta\text{ZPE} - T\Delta S)_B - eU - kT \ln 10 \cdot \text{pH}$$

$$= 1.77\text{eV} - eU - kT \ln 10 \cdot \text{pH}$$

The free energies of the intermediates are plotted in Figure 7 at pH = 0 and 14 for different U values. The rate limiting step, as in the previous case, is the A step, which involves $H_2O + * \rightarrow OH^* + H^+ + e^-$.

5. Discussion

5.1. Oxidation of Water. In Figures 5 and 7, the free energies of the intermediates for the different surface coverages are plotted at pH = 0 and 14 and for different values of the applied potential U.

In these figures, it is shown that to have every step downhill, an overpotential is needed for both covered surfaces. The most favored case is for the totally O covered surface (S^2), which needs an overpotential of 0.78 V ($V = 1.23 + 0.78 = 2.01$) at pH = 0. This overpotential is bigger than for other semiconductor oxides with rutile structures like RuO_2 and IrO_2 (0.37 and 0.56 V, respectively).[47] For the surface with only the bridge sites covered by oxygen (S^1), the overpotential is greater, 0.97 V. However, this overpotential is not really relevant because, at the corresponding value of the bias required for electrolysis (2.20 V), the S^2 surface is stable and not the S^1 surface (section 4.1; see also below). The difference in the overpotential of the rate-limiting step between the S^1 and S^2 surfaces is due to the variation of the local environment among the surfaces, that is, the different occupation of the nearest-neighbor CUSs. The result for S^1 is smaller in comparison with the overpotential of 1.19 V calculated in a previous work.[47] That work did not take into account the peroxo species at the CUS site for TiO_2 that, as was previously reported,[26] is energetically more favorable when there are no excess electrons at the surface (see also section 4.1). For the other catalysts studied in ref 47, IrO_2 and RuO_2, the binding of O at the CUS site is much stronger, and therefore, the original structure used in ref 47 for O* is the relevant structure.

The rate-limiting step, that is, the step with the highest free-energy change, corresponds to the step A ($H_2O + * \rightarrow OH^* + H^+ + e^-$) for both surface terminations. This free-energy difference is 2.20/1.37 eV for the S^1 surface termination and 2.01/1.18 eV for S^2 at $U = 0$ and pH = 0/14.

The inclusion of the peroxo species mentioned above at the CUS sites (the O* intermediate) also changes the rate-limiting step that, without taking them into account (i.e., using O adsorbed to the CUS site without bending to surface O as the intermediate, as in ref 26), would be step B ($HO^* \rightarrow O^* + 1/2H_2$). This result would imply a large surface coverage with the OH* species, in contradiction with experimental results.[8,60,61] Moreover, the most favored step according to our calculations is the D step ($HOO^* \rightarrow O_2 + * + 1/2H_2$). Our results also explain the experimental difficulties in identifying HOO peroxo species on the rutile samples of TiO_2 under conditions where photoexcitation takes place;[60] it should be hard to observe this species since its conversion does not represent the rate-limiting step.

In this work, we have only considered mechanisms involving the CUS site of TiO_2 and no mechanisms involving the bridging oxygen atoms. This can be motivated as follows. At some point, a mechanism involving a surface bridging oxygen atom would have to involve the breaking of one of the bonds of the bridging O atom to a metal atom, making the metal atom available for, for instance, subsequent reaction with H_2O to produce adsorbed OH and $H^+ + e^-$. It is easy to see that the associated free energy for this one-electron transfer step should be higher than the free-energy change for the rate-limiting step in the S^1 and S^2 surface terminations; it would not only involve the dissociation of water into surface-adsorbed OH and $H^+ + e^-$ but also the positive free-energy change associated with the breaking of a $Ti-O_b$ bond. The thermodynamic activation energy should therefore be significantly higher for mechanisms involving bridging O atoms. A similar argument can be made for the reaction of an O_b atom with water leading to OOH and $H^+ + e^-$, for which the associated free-energy change is not much smaller than that for the rate-limiting steps in the S^1 and S^2 surface terminations. For this reason, such mechanisms were not considered in this work.

In Figure 3, we plotted the potential range in which each surface is favored. Comparing these results with the starting

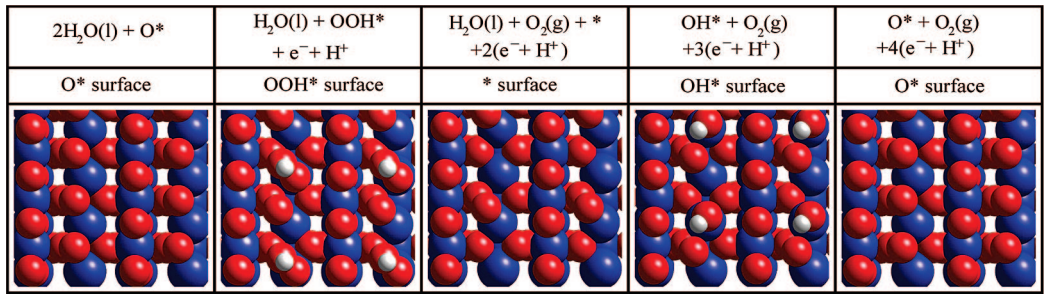

Figure 6. Structures of the intermediates of the oxygen evolution reaction on the O*-covered TiO_2(110) surface (S^2). Blue spheres represent metal ions, red spheres represent oxygen, and white spheres represent hydrogen.

potential for the oxidation of water on the different surface terminations, we can see that, at pH = 0, with the mechanism postulated, oxidation will start to proceed near $U = 2.01$ V, which is the potential needed for the rate-limiting step, A, on the S^2 surface.

Another mechanism including an $O_2H_2^*$ intermediate was also studied for the S^1 and S^2 surfaces. In this mechanism, steps B and C were changed to

$$\mathrm{B}: \ H_2O + HO^* \rightarrow O_2H_2^* + H^+ + e^-$$

$$\mathrm{C}: \ O_2H_2^* \rightarrow HOO^* + H^+ + e^-$$

We found stable $O_2H_2^*$ intermediates for both the S^1 and the S^2 surface terminations. With the computed free-energy changes for steps B and C above, the rate-limiting step was still step A on S^1. In any case, the relevant surface for electrolysis is still the S^2 surface. For that surface, in the mechanism involving the $O_2H_2^*$ intermediate, the rate-limiting step changes from step A to step C, and the corresponding free-energy change increases from 2.01 to 2.18 eV at $U = 0$ and pH = 0. Therefore, although these new steps are possible, we tend to consider the mechanism involving a $O_2H_2^*$ intermediate less important for the oxidation of water on the TiO_2 surface. (The same argument also applies for photo-oxidation, taking into account that S^2 is also the relevant surface for photoelectrolysis).

As stated in section 2, we are working on the assumption that all steps involve one-electron transfer. If we relax this assumption and consider a two-electron transfer process that merges steps A and B, this new step would become the rate-limiting step for both surfaces terminations with overpotentials of 0.605 V for S^1 and 0.69 V for S^2. In this case, and according to Figure 3, it would not be so clear what the relevant surface termination is for direct electrolysis.

5.2. Photo-Oxidation of Water. The difference between the redox potential corresponding to the valence band of TiO_2 at the semiconductor surface under irradiation in contact with H_2O and the O_2 evolution redox potential ($E(O_2/H_2O) = 1.23$ V versus NHE) is assumed to be driving force for the photo-oxidation of water.[62] According to Figure 1, the redox level for the rutile TiO_2 valence band edge is $U_{VB} \approx 3.25$ eV for pH = 0, and this level changes with the pH according to $U_{VB} = 3.25 - 0.059 \cdot \mathrm{pH}$; therefore, $U_{VB} \approx 2.42$ eV for pH = 14.[27,48] (Note that U_{VB} changes with pH in the same way as the O_2 evolution redox potential). According to Figure 3, at the bias potential corresponding to U_{VB}, the rutile TiO_2 surface under intense irradiation is completely covered by oxygen (S^2 surface). Moreover, these values of U_{VB} provide enough overpotential, as shown in Figure 7, for every step in the oxygen evolution reaction; therefore, the photoevolution of O_2 in the TiO_2 anode is thermodynamicaly favorable and kinetically allowed according to our model.

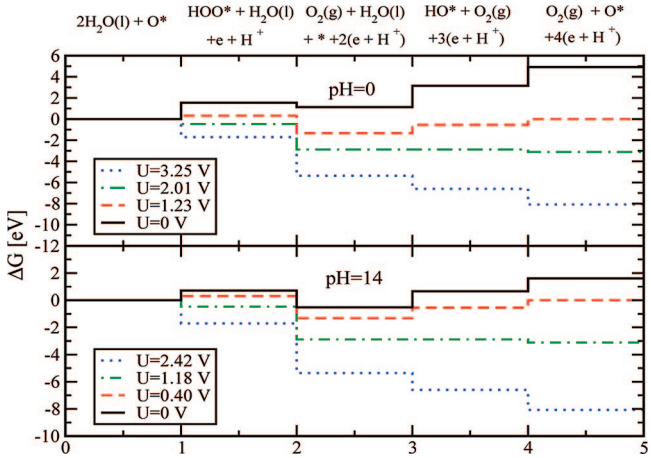

Figure 7. The free energies of the intermediates on the S^2 surface termination of TiO_2 at pH = 0/14 ($U = 0$, 1.23/0.40, and 2.01/1.18 V) are depicted. At the equilibrium potential ($U = 1.23/0.40$ V), some reaction steps are uphill in free energy. At 2.01/1.18 V, all reaction steps are downhill in free energy at pH = 0/14. We also compare to the case with $U = 3.25/2.42$ V the corresponding values of the redox potential versus NHE for the photogenerated holes in the valence band of TiO_2 (rutile) in contact with H_2O under intense irradiation at pH = 0/14.

Our calculations suggest that, with the mechanism studied here, the illumination with light provides enough overpotential for the reaction to proceed at the CUSs. This is in agreement with the experimental results obtained by Nozik.[3] He observed the evolution of H_2 and O_2 at the cathode and anode, respectively, and, from the energy balance for the absorbed photon, estimated the intrisic overpotential available for the photoanode reaction to be between 0.9 and 1.1 eV, after taking into account contributions as, for instance, the band bending and the anodic bias required for hydrogen production. The overpotential calculated here (0.78 V) is less than that available (0.9−1.1 V). Therefore, according to our results and in agreement with experimental findings, in the photoelectrolysis of water using a TiO_2 photoanode, the photo-oxidation of water does not need external assistance; only an anodic bias is needed to reduce the H^+ ions formed to H_2,[3,49,63] which can be done in a tandem cell setup.[34,35]

As in the case of direct electrolysis, we can also consider a two-electron transfer process for the photo-oxidation of water, merging steps A and B. In this case, the overall conclusion is the same; the relevant surface does not change (S^2 surface), and, as the overpotential is lower (0.69 V), the bias potential corresponding to the valence band is still enough to drive the evolution of O_2 in the TiO_2 anode.

6. Conclusions

We have investigated the oxidation and photo-oxidation of water on the ideal rutile $TiO_2(110)$ surface based on the thermochemistry of the reaction steps involved and DFT calculations.

The conclusions are as follows:

(1) Oxidation of water on the $TiO_2(110)$ surface requires a moderate overpotential (0.78 V for pH = 0).

(2) The rate-limiting step for the oxidation process at the CUS sites is $H_2O + * \rightarrow HO^* + H^+ + e^-$.

(3) The relevant surface termination for the photo-oxidation of water is the completely oxygen covered surface (S^2).

(4) The illumination of the $TiO_2(110)$ surface with light provides enough overpotential for the photo-oxidation to proceed spontaneously. It is the wide band gap of rutile TiO_2 that explains the low photoenergy conversion factor of this material.

Acknowledgment. The authors thank Prof. Dr. Jan Augustynski and Dr. Roel van de Krol for useful discussions and suggestions. This research was supported in part by the European Commission (Marie Curie Research Training Network MRTN-CT-2006-032474). This research was also supported by a PIONIER grant for G.-J. Kroes.

References and Notes

(1) Fujishima, A.; Honda, K. *Nature* **1972**, *238*, 37.
(2) Grätzel, M. *Nature* **2001**, *414*, 338.

(3) Nozik, A. J. *Nature* **1975**, *257*, 383.
(4) Jaeger, C. D.; Bard, A. J. *J. Phys. Chem.* **1979**, *83*, 3146.
(5) Nakato, Y.; Tsumura, A.; Tsubomura, H. *J. Phys. Chem.* **1983**, *87*, 2402.
(6) Salvador, P. *J. Phys. Chem.* **1985**, *89*, 3863.
(7) Ferrer, I. J.; Mukaki, H.; Salvador, P. *J. Phys. Chem.* **1986**, *90*, 2805.
(8) Augustynski, J. *Struct. Bonding (Berlin)* **1988**, *69*, 1.
(9) Linsebigler, A. L.; Lu, G.; Yates, J. T., Jr. *Chem. Rev.* **1995**, *95*, 735.
(10) Kavan, L.; Grätzel, M.; Gilbert, S. E.; Klemenz, C.; Scheel, H. J. *J. Am. Chem. Soc.* **1996**, *118*, 6716.
(11) Nakato, Y.; Akanuma, H.; Magari, Y.; Yae, S.; Shimizu, J.-I.; Mori, H. *J. Phys. Chem. B* **1997**, *101*, 4934.
(12) Grätzel, M. *CATTECH* **1999**, *3*, 4.
(13) Shapovalov, V.; Stefanovich, E. V.; Truong, T. N. *Surf. Sci.* **2002**, *498*, L103.
(14) Diebold, U. *Surf. Sci. Rep.* **2003**, *48*, 53.
(15) Carp, O.; Huisman, C. L.; Reller, A. *Prog. Solid State Chem.* **2004**, *32*, 33.
(16) Nakamura, R.; Nakato, Y. *J. Am. Chem. Soc.* **2004**, *126*, 1290.
(17) Nakamura, R.; Ohashi, N.; Imanishi, A.; Osawa, T.; Matsumoto, Y.; Koinuma, H.; Nakato, Y. *J. Phys. Chem. B* **2005**, *109*, 1648.
(18) Takabayashi, S.; Nakamura, R.; Nakato, Y. *J. Photochem. Photobiol., A* **2004**, *166*, 107.
(19) Nakamura, R.; Okamura, T.; Ohashi, N.; Imanishi, A.; Nakato, Y. *J. Am. Chem. Soc.* **2005**, *127*, 12975.
(20) Neumann, B.; Bogdanoff, P.; Tributsch, H.; Sakthivel, S.; Kisch, H. *J. Phys. Chem. B* **2005**, *109*, 16579.
(21) Allegretti, F.; O'Brian, S.; Polcik, M.; Sayago, D. I.; Woodruff, D. P. *Phys. Rev. Lett.* **2005**, *95*, 226104.
(22) Lundqvist, M. J.; Nilsing, M.; Persson, P.; Lunell, S. *Int. J. Quantum Chem.* **2006**, *106*, 3214.
(23) Wendt, S.; Matthiesen, J.; Schaub, R.; Vestergaard, E. K.; Lægsgaard, E.; Besenbacher, F.; Hammer, B. *Phys. Rev. Lett.* **2006**, *96*, 066107.
(24) Nowotny, J.; Bak, T.; Nowotny, M. K.; Sheppard, L. R. *J. Phys. Chem. B* **2006**, *110*, 18492.
(25) Mattioli, G.; Filippone, F.; Bonapasta, A. A. *J. Am. Chem. Soc.* **2006**, *128*, 13772.
(26) Qu, Z.-W.; Kroes, G.-J. *J. Phys. Chem. B* **2006**, *110*, 23306.
(27) Bak, T.; Nowotny, J.; Rekas, M.; Sorrell, C. C. *Int. J. Hydrogen Energy* **2002**, *27*, 991.
(28) Zou, Z.; Ye, J.; Arakawa, H. *Chem. Phys. Lett.* **2000**, *332*, 271.
(29) Zou, Z.; Ye, J.; Sayama, K.; Arakawa, H. *Nature* **2001**, *414*, 625.
(30) Ye, J.; Zou, Z.; Oshikiri, M.; Matsushita, A.; Shimoda, M.; Imai, M.; Shishido, T. *Chem. Phys. Lett.* **2002**, *356*, 221.
(31) Oshikiria, M.; Boero, M.; Ye, J.; Zou, Z.; Kido, G. *J. Chem. Phys.* **2002**, *117*, 7313.
(32) Zou, Z.; Ye, J.; Arakawa, H. *Int. J. Hydrogen Energy* **2003**, *28*, 663.
(33) Ritterskamp, P.; Kuklya, A.; Wüstkamp, M-A.; Kerpen, K.; Weidenthaler, C.; Demuth, M. *Angew. Chem., Int. Ed.* **2007**, *46*, 7770.
(34) Augustynski, J.; Calzaferri, G.; Courvoisier, J. C.; Grätzel, M. In *Proceedings of the 11th World Hydrogen Energy Conference*; Veziroglu, T. N., Winter, C.-J., Baselt, J. P., Kreysa, G., Eds.; Dechema: Frankfurt, Germany, 1996; p 2378.
(35) Augustynski, J.; Grätzel, M. Tandem Cell for Water Cleavage by Visible Light. Patent WO/2001/002624.
(36) Santato, C.; Ulmann, M.; Augustynski, J. *J. Phys. Chem. B* **2001**, *105*, 936.
(37) Khan, S. U. M.; Akikusa, J. *J. Phys. Chem. B* **1999**, *103*, 7184.
(38) Kay, A.; Cesar, I.; Grätzel, M. *J. Am. Chem. Soc.* **2006**, *128*, 15714.
(39) Volodin, A. M. *Catal. Today* **2000**, *58*, 103.
(40) Umebayashi, T.; Yamaki, T.; Itoh, H.; Asai, K. *Appl. Phys. Lett.* **2002**, *81*, 454.
(41) Ohno, T.; Mitsui, T.; Matsumura, M. *Chem. Lett.* **2003**, *32*, 364.
(42) Khan, S. U. M.; Al-Shahry, M., Jr *Science* **2002**, *297*, 2243.
(43) Sakthivel, S.; Kisch, H. *Ang. Chem., Int. Ed.* **2003**, *42*, 4908.
(44) Serpone, N. *J. Phys. Chem. B* **2006**, *110*, 24287.
(45) Paulose, M.; Mor, G. K.; Varghese, O. K.; Shankar, K.; Grimes, C. A. *J. Photochem. Photobiol., A* **2006**, *178*, 8.
(46) Thompson, T. L., Jr *Top. Catal.* **2005**, *35*, 197.
(47) Rossmeisl, J.; Qu, Z.-W.; Zhu, H.; Kroes, G.-J.; Nørskov, J. K. *J. Electroanal. Chem.* **2007**, *607*, 83.
(48) Memming, R. *Semiconductor Electrochemistry*, 1st ed.; Wiley-VCH: Weinheim, Germany, 2001; p 105.
(49) Nozik, A. J.; Memming, R. *J. Phys. Chem.* **1996**, *100*, 13061.
(50) Nørskov, J. K.; Bligaard, T.; Logadottir, A.; Bahn, S.; Hansen, L. B.; Bollinger, M.; Bengaard, H.; Hammer, B.; Sljivancanin, Z.; Mavrikakis, M.; Xu, Y.; Dahl, S.; Jacobsen, C. J. H. *J. Catal.* **2002**, *209*, 275.
(51) Nørskov, J. K.; Rossmeisl, J.; Lagadottir, A.; Lindqvist, L.; Kitchin, J. R.; Bligaard, T.; Jónsson, H. *J. Phys. Chem. B* **2004**, *108*, 17886.
(52) Atkins, P. W. *Physical Chemistry*, 6th ed.; Oxford University Press: Oxford, U.K., 1998; pp 485, 925−927, and 942.
(53) Bullard, J. W.; Cima, M. J. *Langmuir* **2006**, *22*, 10264.
(54) Payne, M. C.; Teter, M. P.; Allan, D. C.; Arias, T. A.; Joannopoulos, J. D. *Rev. Mod. Phys.* **1992**, *64*, 1045.
(55) Hammer, B.; Hansen, L. B.; Nørskov, J. K. *Phys. Rev. B* **1999**, *59*, 7413.
(56) Vanderbilt, D. *Phys. Rev. B* **1990**, *41*, 7892.
(57) An open source code available at http://wiki.fysik.dtu.dk/ase.
(58) Hammer, B. Private communication.
(59) Matthey, D.; Wang, J. G.; Wendt, S.; Matthiesen, J.; Schaub, R.; Lægsgaard, E.; Hammer, B.; F.; Besenbacher, F. *Science* **2007**, *315*, 1692.
(60) Augustynski, J. Private communication.
(61) Howe, R. F.; Grätzel, M. *J. Phys. Chem.* **1987**, *91*, 3906.
(62) Nozik, A. J. *Annu. Rev. Phys. Chem.* **1978**, *29*, 189.
(63) Tomkiewicz, M.; Fay, H. *Appl. Phys.* **1979**, *18*, 1.
(64) Lindan, P. J. D.; Harrison, N. M.; Gillan, M. J. *Phys. Rev. Lett.* **1998**, *80*, 762.

JP711929D